Presented at the Second Int. Conf.
on Ion Sources, Vienna, Austria,
September 11-16, 1972

LBL-1219

PERFORMANCE CHARACTERISTICS OF A COMPACT SELF HEATED CATHODE SOURCE AND ANALYZER FOR THE BERKELEY 3-MV SUPERHILAC INJECTOR

Basil F. Gavin

August 1972

AEC Contract No. W-7405-eng-48

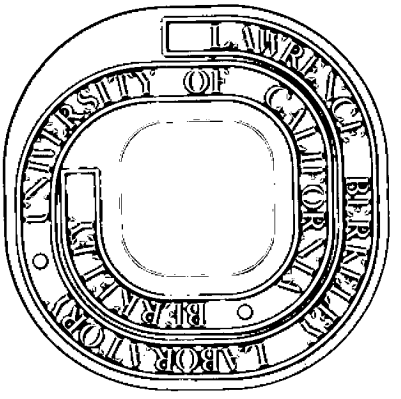

LBL-1219

DISCLAIMER

PERFORMANCE CHARACTERISTICS OF A COMPACT SELF HEATED CATHODE SOURCE AND ANALYZER FOR THE BERKELEY 3-MV SUPERHILAC INJECTOR*

Basil F. Gavin

Lawrence Berkeley California
University of California
Berkeley, California

Abstract

A PIG discharge, designed for the production of multiply charged ions for operation in the Berkeley SuperHILAC 3-MV injector and operating in a magnetic gap of 5.8 cm at 2000-4500 gauss, has been studied in conjunction with and inseperable from a 123° analyzer. Results here reported were made with a test magnet. Analyzed ion beams have been rendered by varying beam energy, and magnetic field of both analyzer and source. Inert gaseous ion yields are reported, as are the ion source arc characteristics. A fast pulsing gas valve is also described.

Effort has been directed towards the ionization of solid materials to a charge to mass ratio of ≥ 0.04. 7.2μA of gold^{10+} and at least 11μA of germanium$^{4+}_{76}$ has been analyzed and measured.

1. Introduction

Recent work at the SuperHILAC source test facility has been directed toward the making of a germanium ion beam. The ion source and 3-MV terminal for the SuperHILAC is described in reference 1. Ions to be accelerated will have a charge to mass ratio (ϵ) of $\geq .046$, and the source runs at about 24% duty factor. A sputtering type of atomic particle feed, an attractive approach for pulsed sources, was selected[2,3] for germanium and other solid materials.

Limits on the amount of power consumed in the 3-MV terminal were imposed at an early date. The terminal source magnet at full field uses 2400 watts and weighs 480 lbs. A bending radius of 14 cm. with a turning angle of 129° and a magnet exit (effective) field edge-angle of 32°, provides for sufficient charge state separation after analysis. A $\Delta\epsilon/\epsilon$ of about 3% given a 1.3 cm aperture is realized with this geometry.

Results reported here were made with a test magnet differing magnetically in small degree from the magnet used and reported on in reference 1[4]). The compact 840 Hz electronics for the 3-MV terminal source were not used, nor were the two cold fingers that cryopump the terminal vacuum system.

The magnetic field on the source axis is designed to exceed 4000 gauss at optimum running conditions and at lowest acceptable charge to mass ratio. This limit serves to minimize the ampere turns requirement of the magnet. Observe that this is a 'low field magnet' since at higher charge to mass ratios and modest extraction potentials (U), source fields are singularly low. [For example: with an ϵ of .058, U = 12KV; B (source) = 2700 gauss.]

Emittance measurements have not been made for the metallic beams reported here. Prior results with argon show an axial and

*Work performed under the auspices of the U. S. Atomic Energy Commission.

radial area of 20π and 31π cm-mrad (90% contour) respectively at the entrance to the accelerating tube. (U = 16 KV).

Beam currents (I_m) will be reported as electrical current and will be for peak values. Beams are measured in a large faraday cup (with magnetic trapping) at close to the radial focal point of the beam. See fig. 1. Ion species are separable only with tight collimation proceeding this cup. The magnetic field in the analyzing gap is swept through a range of from 3800 gauss to 7800 gauss. By necessity the field on the source axis (~ 0.6 x B_z analyzing gap) follows this change. Arc characteristics begin to appreciably alter when fields in the magnet drop below 4500 gauss (2700 at source). Further discussion is forthcoming. See fig. 4.

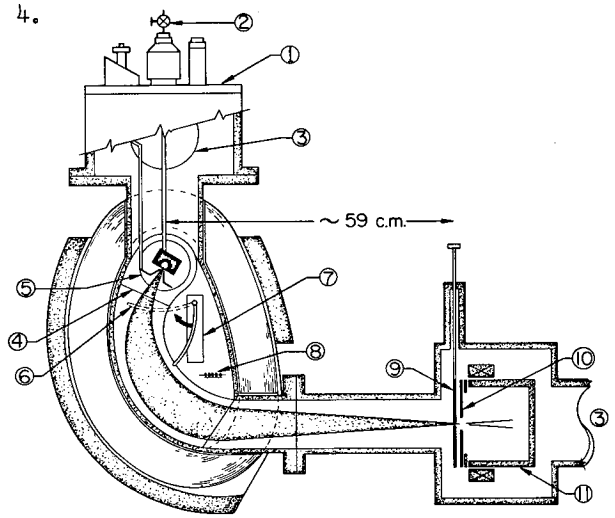

The plan view shows: 1) ion source; 2) leak valve; 3) two 6" diffusion pumps; 4) step in the magnet pole from 7.4 cm. gap on the ion source side to 3.6 cm. gap; 5) extractor; 6) calorimeter; 7) 15 junction thermopile; 8) ion gauge; 9) 4 x40mm collimator; 10) 13 x50mm collimator; 11) faraday cup.

Figure 1

Full coverage of the ϵ range necessitates operating at low fields for the highest charge states, and in some cases a change in beam energy. An attempt to hold the ion flux from the plasma constant was effected by adjusting the anode to extractor gap (d) for constant space charge limited conditions as derived by Chavet[5]). A gap gradient of 100KV/cm at 20KV is considered a productive, practicable gradient. Following this condition, actual gradients vary from 77KV/cm (U = 7KV) to 104KV/cm (U = 24KV) for a derived angle of convergence of from 8° to 9.7° respectively.

When beam energy was altered, the extractor position across the slit was tuned for maximum ion current with minimum collimation downstream. Slight adjustments were always required for differing potentials and also with the passage of time. Gas flows and arc currents were kept constant during any scan of source productivity, unless otherwise noted.

The average charge state of an ion source output is defined as: $\bar{q} \equiv I_m^{Total} / I_p^{Total}$. I_m^n = measured peak current in μA, of charge state n, I_p^n = particle current in μA. $I_p^n = I_m^n / n$ and $I_p^n = I_m^n \times 10^{-6} / ne$ = peak particle flux. I_m^n is measured by reading the separate peak currents passing through a slit collimator. In cases where Ip could not be measured for all values of n, these particle currents were estimated from a plot of I_p^n and verified by changing extraction potential under the constant ion flux condition mentioned above. An integration of these peaks is meaningless, since the beam is being swept across a fixed slit. Collimator size therefore becomes an important performance parameter.

Two collimator sizes are used herein, the small 4 x 40mm slit as an aid in identifying ion species, the larger 13 x 50mm to estimate, yet separate peak ion currents that could be achieved without collimation. This larger collimator was chosen to allow the light and medium weight ion species to be separated from each other. When both

collimators are removed, beam levels for the easily separated isotopically pure ions are approximately twice as high then when the larger 13 x 50mm slit is used. The state of collimation therefore will always be reported. Realize that distortion from 180° analyzer data is evident due to 1) the changing angles of convergence through the extractor caused by varying (extractor anode gap (d), 2) neutralization and beam blow-up through the analyzing magnet, and 3) varying, sometimes marginal, field conditions on the source axis. In spite of these limitations the practical nature of the results warrant statement.

2. Source Design & Description

It can be pointed out now, as supplementary information to ref. 1 that the recessing of the cathodes into the pole pieces, while causing a bowing of the magnetic field lines in the cathode vicinity, does not seem to appreciably deter the beam productivity of argon, up to Ar^{6+}. Tests were run with three conditions of cathode penetration (zero, .35, and .7 cm). Deeper penetration has yet to be explored. See fig. 2. The anode now in use is made from copper and is freon cooled to minimize hydrogen loading of the cryopumped terminal vacuum system. The bore of the anode may be cleaned from sputtered cathode material with a tapered reamer and a dental sandblaster. A removable window plate is incorporated and penetrates the plasma 0.2 mm. A window size of 8 mm x 1.25 will be used unless otherwise noted.

The test magnet is pumped differentially by two 6" oil diffusion pumps. Speeds of 500 ℓ/sec (air) are measured at about the center of rotation of the magnet analyzer. A simple needle valve controls the gas flow which is monitored by a commercial instrument.

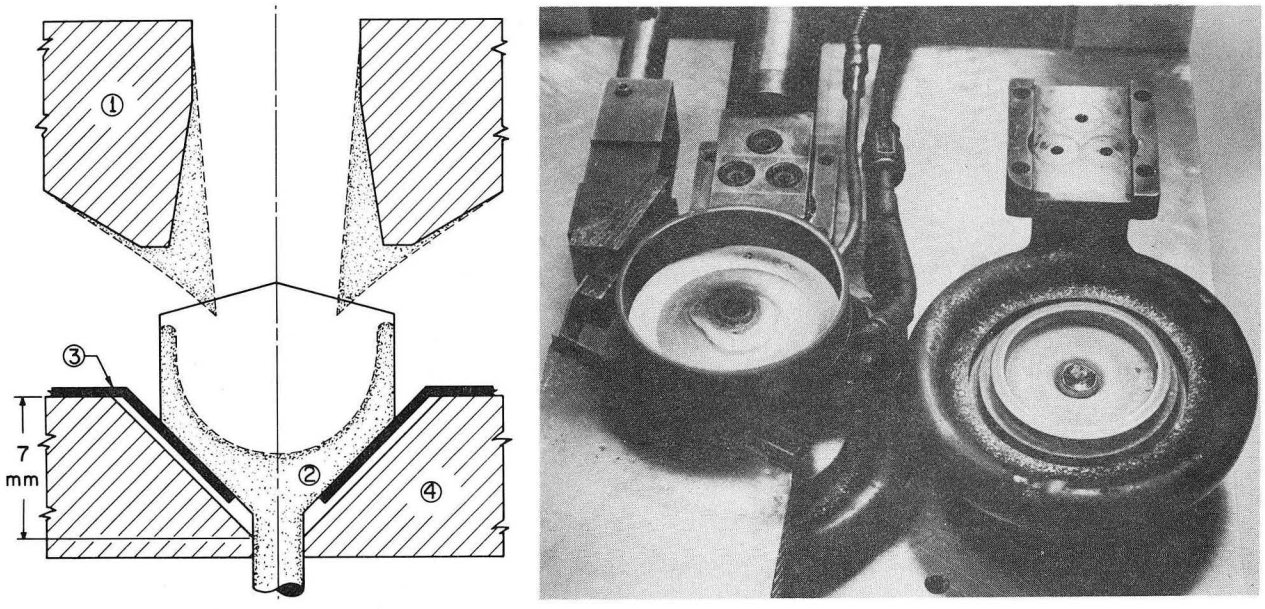

View of cathode vicinity after running. Quartz ring spacing insulator coated with tantalum. Cross section of cathode and immediate vicinity shown at left. 1) anode; 2) tantalum cathode; 3) heat shield; steel cathode boat, shaded area shows cross section of tantalum build-up after running.

Figure 2

No effort has been made to halt secondary electrons created at the extractor from reaching the ion source. Optimum performance is obtained when some ions from the anode window strike the 'outside' jaw of the extractor as evidenced by a sputtering wear pattern. A vertical divergence pattern of $\pm 9^{\circ}$ is engraved on the extractor jaws. Long 'dee' plates extend into the analyzing gap and generate a field free region for the beam to pass through.

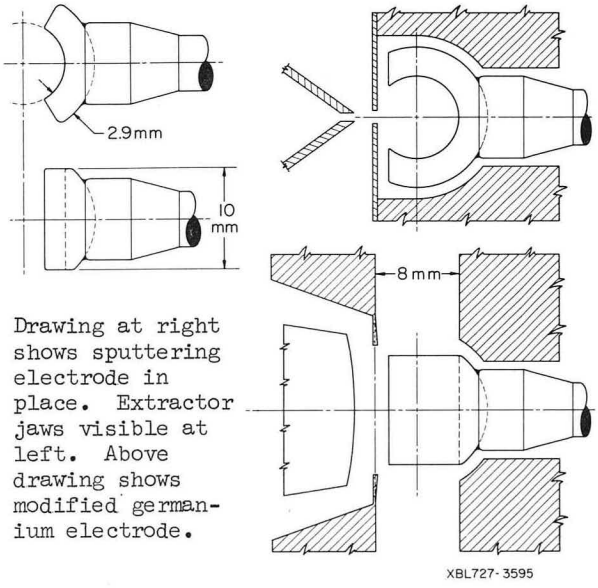

Drawing at right shows sputtering electrode in place. Extractor jaws visible at left. Above drawing shows modified germanium electrode.

Figure 3

The sputtering electrode is biased negatively with respect to the plasma potential with a 1 KV, 0.8 amp DC supply, and is in series with a 100 ohm current limiting resistor. The electrode is spherical in shape so as to maximize the surface area adjacent to plasma. This therefore allows sputtered material to be recycled, in as much as the escape area from the ball represents but three quarters the total surface being sputtered ($1.9\ cm^2$). The ball electrode lies directly behind the anode window (see fig. 3). When feasible a freon cooled copper stem is soldered to the material to be sputtered. Germanium proved to be a challenging element to cool since it is easily fractured when under heat shock[†]. Consequently, only a section of full ball would hold together when sputtered by the arc. See fig. 3. One half the working area of a full ball electrode, and an unfavorable trapping geometry, must be accepted.

4. Operation

This pulsed ion source runs in its positive resistance mode with maximum available voltage (4.5KV) until the power consumed causes the cathodes to emit electrons thermionically and makes possible operation in the high current, negative resistance mode. (Supranormal gas flows and magnetic field aid in rapid striking of the arc). The gas flow may then be lowered, and, typically runs between 0.03 to 0.15 cc/min. For metallic ion production it is essential to operate at minimum flow. Care must be taken to quickly supply this arc with greater gas flow should accidental sub-minimal flow be assumed. Test stand gas flow adjustments were made by hand but for terminal operation, a gas control system is described in the Appendix. An alternative method for striking the arc is to raise the duty factor of the applied potential across the arc. For example, at 32% duty factor with but 2KV across the arc, it will just develop enough power in the arc to strike same. Once struck the duty factor can be lowered as a means of increasing the arc potential (V),

[†]As molybdenum has a coefficient of expansion close to that of germanium, a cooled molybdenum stem was first lapped to close fit a single crystal germanium ball, flash coated with 500 A° of palladium, and then recoated with about 2 microns of gold. After heat treating same to 800° C, a 30 micron gold foil was sandwiched between molybdenum and germanium, and then raised in temperature to about 380° C so as to slightly exceed the 350° C eutectic of germanium/gold.

for best multiply charged ion output. Of course balanced against this are the benefits of increased duty factor. Longer cathode life at lower duty factors is not insured since greater arc potential (V) leads to greater sputtering rates. (An interesting empirical formula for this rate is given by Pasyuk[6]) for tungsten). Given the cathode geometry shown in fig. 2, a 24% duty factor gives us proper cathode emission and a satisfactory range for a 2-4 amp current regulated supply. Tantalum cathodes† are at present

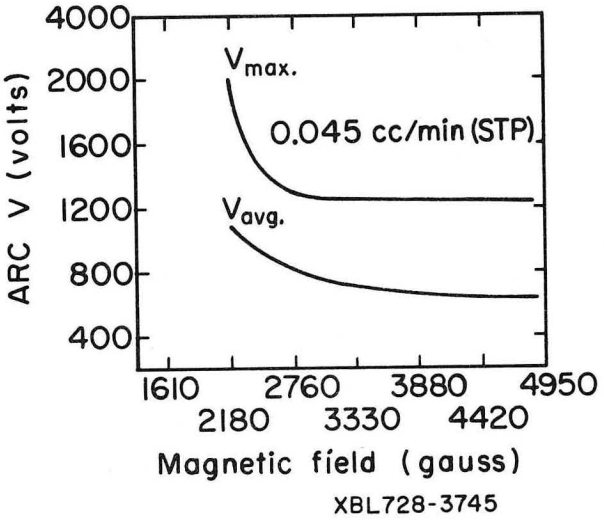

3 amp Krypton arc (24%). Magnetic field measured on centerline of source axis. V_{max} = peak arc potential at beginning of pulse. V_{avg} = average arc potential.

Figure 4

used and give us an eight hour lifetime with a 2.4 ampere, 24% arc; about 0.53 gms/hour builds up on the anode as shown in fig. 2. Curves showing arc potential as a function of magnetic field are displayed in fig. 4, and while typical, will constantly change with ion source age, duty factor, arc current and gas flow! Should V_{max} not be available at the arc, a delay of several milliseconds will take place during the pulse before the negative resistance characteristics set in.

A calorimeter may be pivoted into the analyzing gap at the pole step position. If all the ions are collected on the calorimeter, I_m^{Total} can be measured†. With an 80KV/cm gradient between extractor and anode, 29mA/cm^2/amp is a good figure of merit for this source.

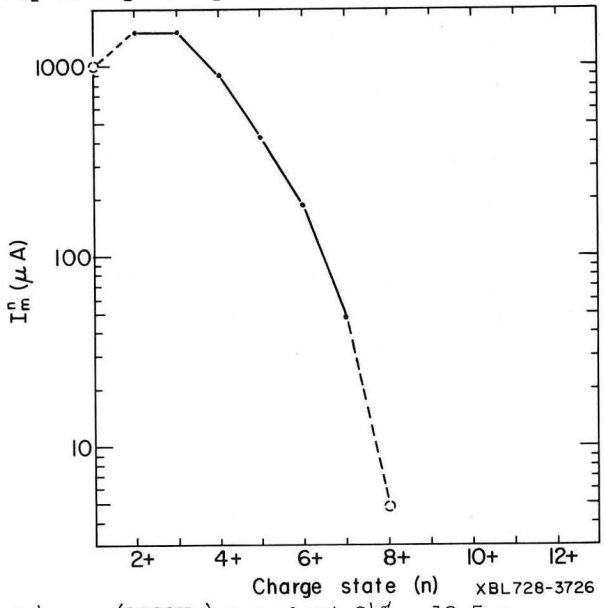

2.4 amp (1200V.) arc about 24%. 13.5 x 1.25mm. window. 0.13 cc/min. (STP) argon gas flow. No collimation extractor/anode gap 1.5mm, U = 21KV Ar^{+1} estimated.

Figure 5

†Titanium cathodes can be used to real advantage for lower duty factor, cold cathode operation, providing they are soft soldered to the cathode steel boats. A 2 amp, 24% (1050V) arc may be run. Up to 4 amp (1180V) is feasible at lower duty factors (8%). Such high currents are not available from 'cold' tantalum cathodes, i.e., operation at say 2 amp at 8% duty factor for longer source life can only be attained with titanium (or V, Ni); not with tantalum or tungsten.

†Calorimeter measurements will not yield average charge $\bar{q}$ but serves well for measuring total beam currents (I_m). Defining duty factor as To/T where To is pulsed width, T repetition period, peak power = measured power/To/T, measured power (watts) = $\frac{To}{T} \sum P_n = \frac{To}{T} \sum (nUeI_p^n) = \frac{To}{T} U I_m^{Total} \times 10^{-6}$ where P_n = power from individually charged species. A thermopile close to the calorimeter is used to measure the temperature difference between ingoing and outgoing water. Equilibrium readings may be taken within sixty seconds.

36mA/cm.^{2}/amp is typical with 120KV/cm gradient given the anode window area in cm^2 and arc current in amps. These measurements were taken at the outlet of the source dees eleven cm. downstream from the source. Prior measurements show about 20% more current immediately following the extractor. When the gradient is scaled (following Chavet's derivation), ion current remains constant to within a few percent. About a quarter of the extractor power supply current drain appears due to secondary electron loss to the ion source for potentials greater than U = 8KV. Since I_m^{Total} does change with gas flow, I should mention that these figures of merit are taken at minimum gas flow.

5. Performance

The SuperHILAC will accelerate Ar^{2+}. A one amp cold cathode arc will suffice. Fig. 5 illustrates the best uncollimated beams of argon that can be expected to date. $I_m^{Total} \simeq 5.5$ mA of argon, $\bar{q} \sim 2.1$. A top gradient of 138KV/cm is employed. 12 ma/cm^2/amp of argon ions leave the analyzer magnet, about 30% of the measured beam at the extractor. Ar^{8+} was analyzed with but 1900 gauss on the source axis. As the arc ages and for reasons not understood, the arc sometimes will not run below 2400 gauss without inordinate increase in gas flow. Therefore at U = 21KV, ions of greater charge than Ar^{4+} cannot be depended upon.

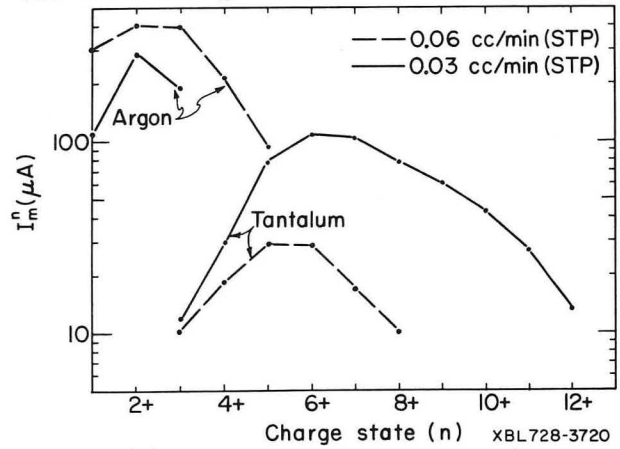

3 amp, 24% argon arc, U = 12KV, 100KV/cm gradient. 13x50mm collimation.

Figure 6

Tantalum ions are readily taken from this arc possibly because the median plane of the beam line is but 2.3 cm from the cathodes. Results with two gas flows are shown in fig. 6, using the 13x50mm. collimator. $\bar{q} = 6.5$ for this lowest allowable flow rate condition. Notice that while tantalum appears to dominate the arc, in fact 90% of the particles that leave the source are gaseous argon. Fig. 7 shows tantalum output as a function of arc current.

The isotopes of krypton and most of those of xenon may be separated with the 4x40mm collimator slit. The yields of Kr_{84} and Xe_{129} are given in fig. 8. In the case of krypton it is possible to sum the individual isotopes for a total krypton beam. The average charge $\bar{q}$ for krypton is 2.3 and for xenon $\bar{q} = 2.9$ (extrapolating Kr^{+1}, $Xe^{+1,2+}$). Bear in mind that the shape of these performance curves will change. The greater the extraction potential, the less favorable or larger will appear the charge state ratios

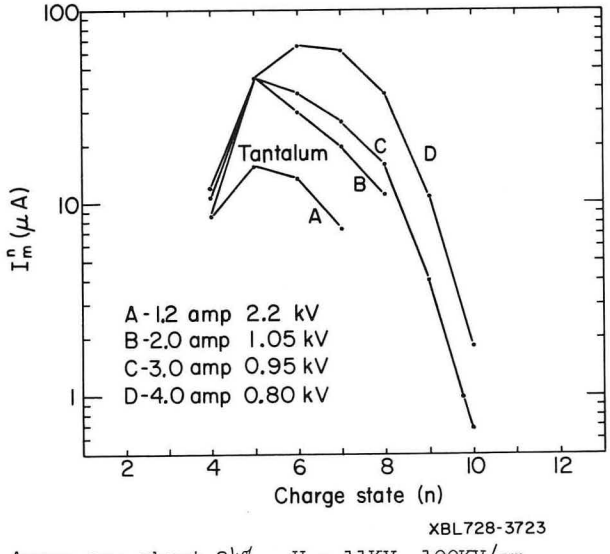

Argon arc about 24%. U = 11KV, 100KV/cm. 4x40mm collimation. Gas flow unrecorded.

Figure 7

even though beam levels rise, since the lower charge states will experience greater loss from space charge blowup at low energy in the analyzing magnet.

The metallic ions are optimized by varying the potential between sputtering electrode and anode, (ΔV). A full size gold ball electrode is illustrated in fig. 9 with the window plate removed. Approximately 40% of the sputtered gold may be salvaged from this window plate, the remaining material depositing above and below the ball or lost in the beam. The internal diameter of the electrode increases in diameter at about 4μ/minute (ΔV = 250V, 2.8 amp, 24% arc). At this rate the gold should last about fourteen hours. Tantalum will rapidly cover the inner surface of this electrode when this surface is not being sputtered. A factor of two increase in the lower charge states of tantalum is noticed when $\Delta V < 50$ volts.

The relation between gold ion yield and ΔV has been explored with gold and is shown in fig. 10. All parameters except magnetic

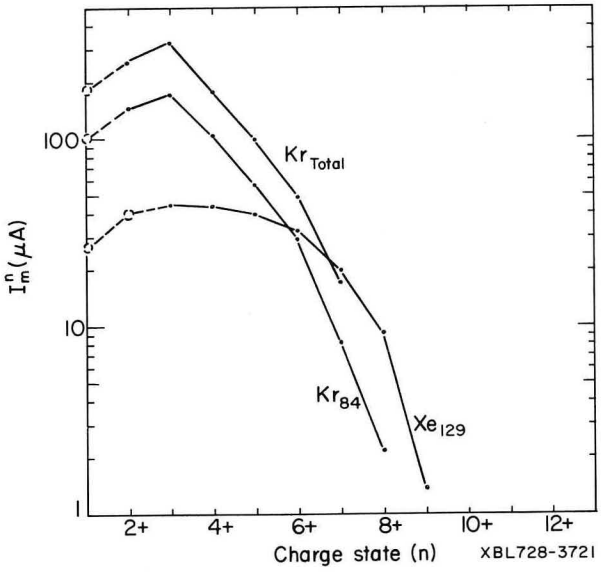

2.9 amp arc at 24%. U = 16KV, 100KV/cm. 4x40mm. collimation. Gas flow unrecorded. Kr^{+1}, Xe^{+1}, Xe^{2+} estimated.

Figure 8

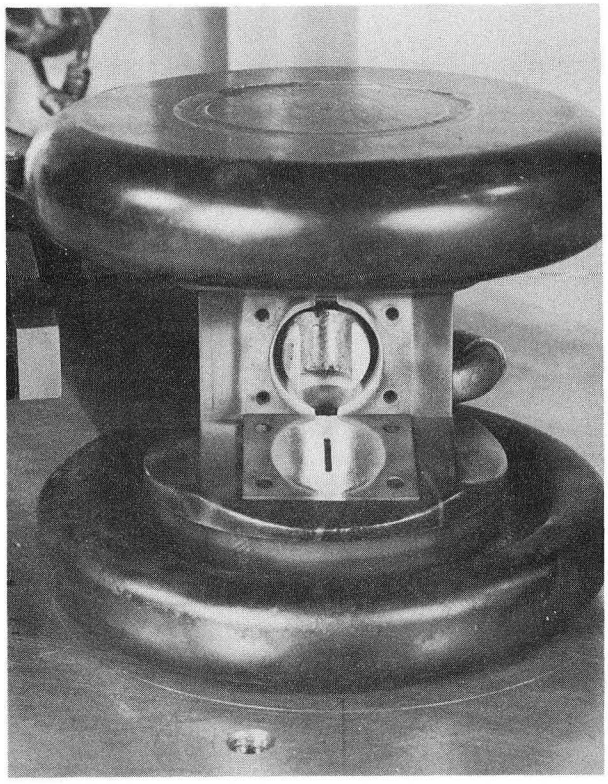

Ion source, less extractor. Gold electrode in place.

Figure 9

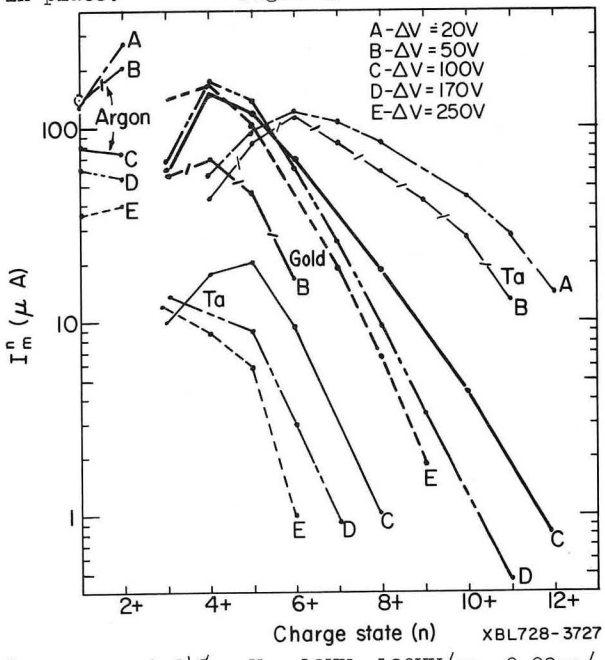

3 amp arc at 24%. U = 12KV, 120KV/cm. 0.03cc/min argon, (STP). 13x50mm collimation.

Figure 10

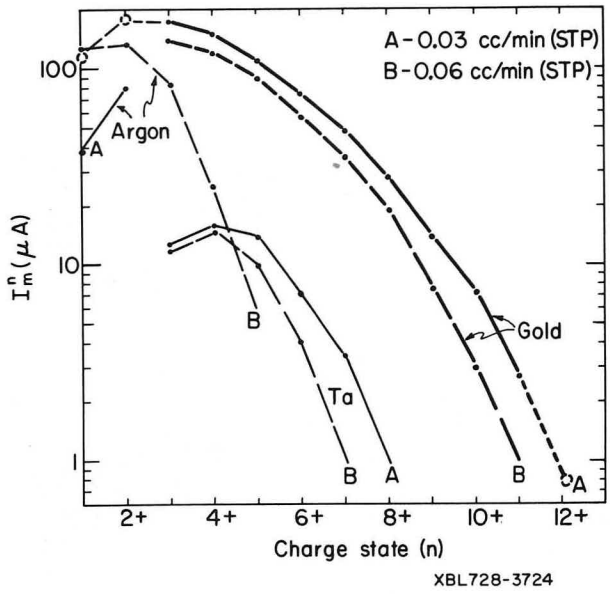

3 amp argon arc at 24%. U = 12KV, 120KV/cm. $\Delta V \simeq 110V$, I_s = 0.6 amp ± 0.1. 13x50mm collimation.

Figure 11

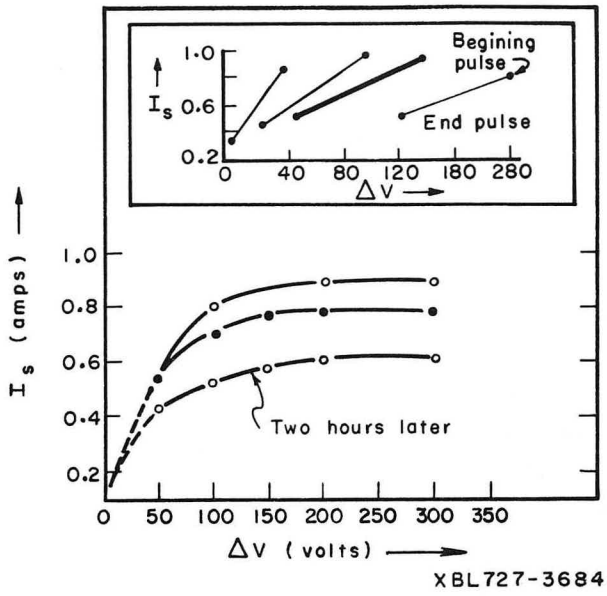

Sputter electrode bias vs. electrode current. Insert illustrates voltage/current changes with time.

Figure 12

field were kept constant. Argon and tantalum production vs. ΔV are displayed in light line. (Data presented in fig. 6 was taken simultaneously with that of fig. 10 but with ΔV = 0). Fig. 11 shows the support gas flow parameter effect on metallic gold ion yield. Notice that the apparent charge state ratios of tantalum and gold are uneffected by this pressure change. The parameters are tuned for best gold^{10+} yield. Estimating $Au^{+1,2+}$, $\bar{q}$ for gold = 2.6. Approximately equal numbers of gold and argon ions leave the source.

Extraction potentials have unfortunately been limited to values less than 16KV since a voltage breakdown problem has not yet been solved on the cooling lines of the sputtering electrode. Improved beam levels are expected with greater extraction energy. The arc current effects the yield of gold in a manner shown by the curves for tantalum seen in fig. 7, but to a lesser degree. Greater arc currents require a slightly greater potential difference between anode and electrode. Gold beams appear to be optimized when ΔV = 110V. Figure 12 shows (at three amperes arc current) electrode current (I_s) -vs- ΔV electrode volts. I_s reaches a near constant value that is set by the surface area of the electrode, the sputtering yield, and the distance between this surface and the active plasma. In truth ΔV given here is an average value, varying as shown on the insert of fig. 12. In time, these curves uniformly drop in amplitude creating a family of curves. A slight increase in ΔV is believed to be required as time passes for optimum gold production. In any event, gold beams decrease steadily in time to about 50% maximum value during the lifetime of the tantalum cathodes.

Niobium ion output is shown in fig. 13. The niobium electrode is a full ball as with gold. The output of niobium has not been optimized due to current limitations of the sputtering supply. A greater ΔV might be called for. $\bar{q}$ for niobium is 2.4; for argon with sputtering on and off, 1.7 and 1.9 respectively. About equal amounts of the

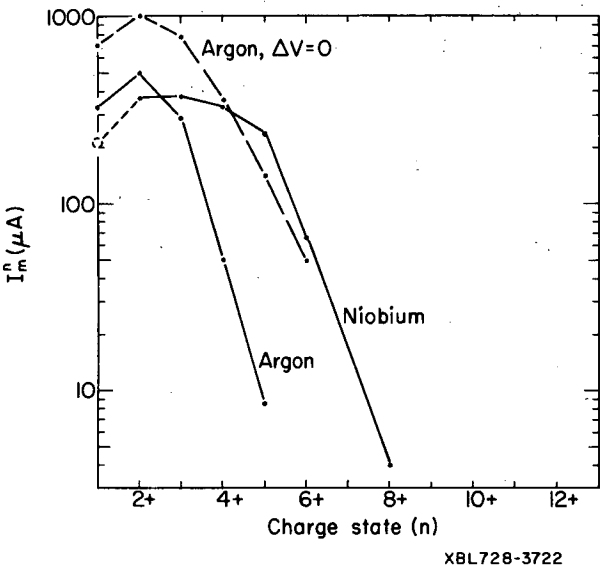

2.6 amp argon arc at 24%. U = 16KV, 100KV/cm. ΔV = 500V, I_s = 1.3 amp. Nb^{+1} estimated. Gas flow unrecorded.

Figure 13

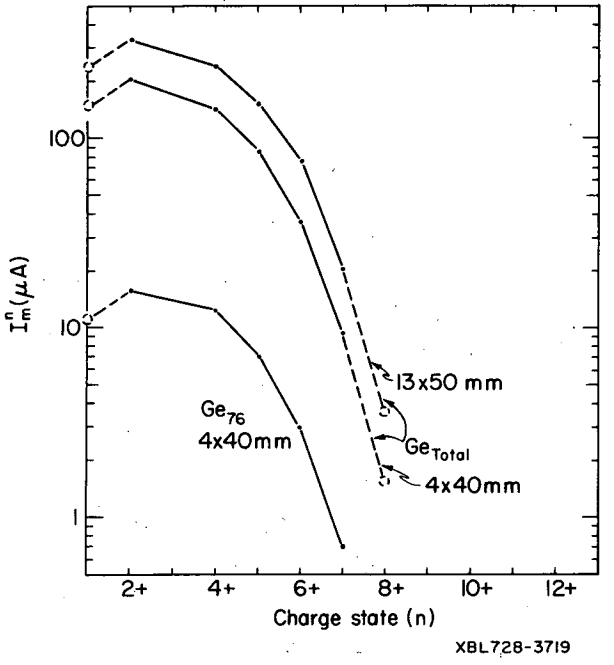

2.8 amp argon arc at 24%. 16KV, 100KV/cm. ΔV = 700V, I_s = 0.3 amp 0.5cc/min. (STP).

Figure 14

metallic and gaseous ions are present in the beam. Whether sputtering is on or off, I_m^{Total} = 2.9mA (.34mA of Ta). About 12.5mA/cm^2/amp of ions leave the magnet; a figure of merit for source and analyzer. Nb^{+1} is estimated from a lower energy run.

The SuperHILAC will accelerate germanium $^{4+}_{76}$. Beams of 2.8 particle microamperes (peak) have been separated and measured from natural material using argon as a support gas and the smaller 4 x 40mm. slit. Separated Ge_{76} and a summing of all isotopes (Ge_{Total}) may be seen in fig. 14. A change to the larger collimator alters total beam levels as shown, but can only approximate actual beam currents since all the isotopes of germanium are not separated. The average charge $\bar{q}$ for germanium is 2.2.

Due to the tendency of this material to crack from temperature drop across the sides of the ball, the short modest electrode shown in fig. 3 was chosen. A ΔV of 700V has not yet been exceeded. Optimum performance therefore might not have been reached. The sputtering yield of germanium with 500 eV argon ion energy is half that of gold (2.4)[7], the yield of niobium, one quarter. Consequently it is likely that the greater potential called for in the case of germanium and niobium, acts as a reaching out for a specific atom/ion yield that is in proportion to the sputtering yield of the material.

7. Discussion

The importance of excellent vacuum conditions for multiply charged ion sources has not been mentioned. Typical operating pressures are from 5 to 10 x 10^{-6} mm Hg. Charge exchange is an important factor and must be recognized even at these pressures. A more detailed discussion may be found in ref. 1.

Longer cathode life is sorely needed.

Deeper penetration into the steel cathode 'boats' (fig. 2) will be explored. However the tight constriction of the anode from built up tantalum waste would seem to limit this solution's practicability. Operation at lower duty factors will lengthen life time providing cathode temperatures may be more readily reached for secure thermionic emission and therefore lower arc potential drop. Cold cathode operation, possibly with titanium, will allow the SuperHILAC terminal to lower source duty factor for longer life, high current operation.

cathodes are made from pressed tantalum powder mixed with gold powder (66% by volume Tantalum), the following spectrum was recorded as shown in fig. 15. A 2 amp 24% arc had 60% normal impedance. After a short bake-out period, gold ions were extracted with excellent charge state ratios. The effect was short lived. Apparently the gold wicked to the surface before vaporizing and/or sputtering away. With exception of small pockets of yellow colored cathode material, most of the gold was removed within 15 minutes of running, following bake-out.

Table 1

Element^{n+}	Argon^{2+}	Krypton$^{4+}_{Total}$	Ge$^{4+}_{Total}$	Niobium^{5+}	Xenon$^{7+}_{Total}$	Gold^{10+}
Measured (μA)	1500 (No Coll.)	180 (4x40)	140 (4x40)	240 (13x50)	77 (4x40)	7.2 (13x50)
Extrapolated (μA) To 13x50 Coll.	800	~330	~260	240	~140	7

The performance figures, measured and already stated are given in Table 1. Xe_{Total} is implied from measurements of Xe_{129}. In the interest of knowledgeable summarization and realizing possible error in extrapolating from small to large collimation, i.e., for Ge, Kr and Xe, the beam levels expected through 13x50mm collimation are also given in Table 1. The average charge, crudely calculated from these data shows a maximum value for xenon at 2.9 and a minimum for argon at 2.1, with the exception of 6.5 for tantalum from the cathodes. Realize that $\bar{q}$ will vary with extraction potential and arc current, and that greater transmission efficiency in the analyzing magnet should lower $\bar{q}$. Also note that the average charge of the metallic ions appears to be insensitive to small changes in gas flow.

An interesting alternative method for introducing metallic material into the arc was briefly explored. If the tantalum

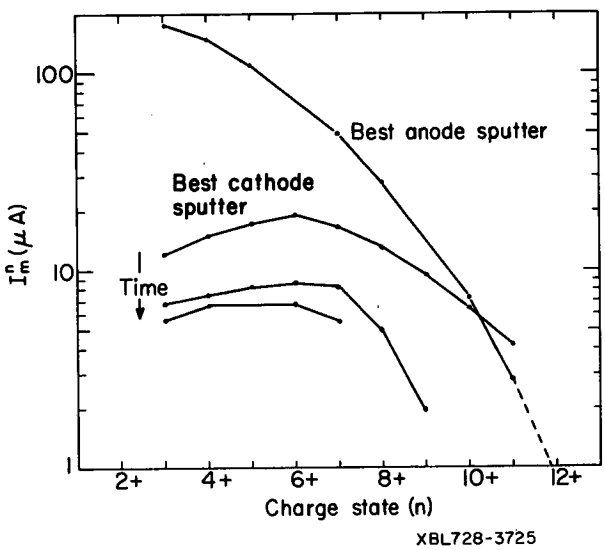

Gold ion yield. Best anode sputter taken from fig. 11. Three sets of data were taken over a 15 minute period for best cathode sputter. 2.1 amp argon arc at 24%, 0.14cc/min (STP). U = 12KV, 100KV/cm.

Figure 15

A thought comes to mind that the material to be sputtered away could be encouraged to wick from reservoir to surface for either the

cathodes of the arc or sputtering electrode. Careful temperature control of a porous, refractory carrier would be required. The high $\bar{q}$ for tantalum and implied $\bar{q}$ for gold ions from the cathode compares well to the $\bar{q}$ of gold from the sputtering electrode. The close proximity of the cathodes to the anode window gives this source access to ions that in a longer source would be lost to the walls in accelerated fashion.

8. Appendix

A metered amount of gas (10^{-3}cc, STP) may be dumped into the source within fifty milliseconds, upon command, triggered by a detected abnormal increase in arc potential across the arc. This gas pulse is stretched out over a period of about a quarter of a second. The valve used is made by taking two miniature solenoids and placing them back to back, tieing their seats together with capillary tubing (19mm x 0.13mm, inner diameter) and then pulsing first that solenoid nearest the source with a 32 volt, 16 millisecond pulse. See fig. 18. For normal gas control we use a commercially available thermo-mechanical leak valve, highly suitable for our high pressure environment since the valve is built into a small pressurized gas reservoir, but because of slow response time with this drawback, when the arc impedance is rapidly changing and needs to be lowered. Input pressure to the double solenoid may be as high as 170 pounds/in^2 given the springs supplied with the commercially available solenoid. If greater pressure is applied, #1 solenoid will not fully seal. Consequently the input to #2 solenoid can be connected to the gas reservoir providing its pressure is below 170 pounds. An open loop servo works as follows: the detector looking at arc potential signals for a gas burst with one or more counts over an interval of ten since arc

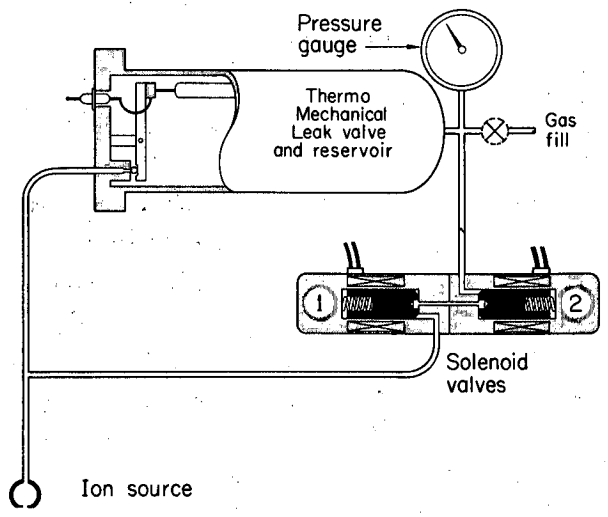

XBL727-3594

Block diagram of gas control system.

Figure 16

starvation is first observed by either potential spikes, or a sudden permanent increase in impedance during any pulse. #1 valve is opened. Several seconds later #2 valve opens to recharge the capillary tube, followed by an incremental increases in the leak rate of the thermo-mechanical leak valve. The process continues until the slow mechanical leak valve is operating at correct flow.

Acknowledgements are extended to D. Spence and W. Hansen for their suggestions and also to W. Elwood for excellent work.

References

1) D. A. Spence, B. Gavin, et. al., "A 3-MV Injector for the SuperHILAC," paper at the 1971 Particle Accelerator Conference (also UCRL-20452, LBL, Berkeley, California

2) B. Gavin, "A Sputtering Type Penning Discharge for Metallic Ions," Nuc. Instr. and Methods 64 (1968) 73-76 (also UCRL-18082, LBL, Berkeley, California

3) Yu. P. Tret'yakov, A. S. Pasyuk, et. al., Atomnaya Energiya, 28, No. 5 (1970); JINI preprint P7-4477, Dubna, 1969

4) The test magnet has a bending radius of 15.6 cm and a 123° angle of analysis. The terminal magnet has a bending radius of 14.2 cm and a 129° angle of analysis. The latter magnet shows signs of saturation at 0.7 x full held strength. Consequently the test magnet analyzing gap field is 11% higher at ninety amperes (8200 gauss)

5) I. Chavet, "Ion Extraction and Beam Formation from a Plasma Ion Source," paper at the 1970 Marburg Electromagnetic Isotope Separators Conference, P. 313

6) A. S. Pasyuk et. al., PTE, No. 3 r2 (1965); JINI preprint 1644, Dubna, 1964

7) G. Carter and J. S. Colligon, "Ion Bombardment of Solids," London, 1968, P.323

TECHNICAL INFORMATION DIVISION
LAWRENCE BERKELEY LABORATORY
UNIVERSITY OF CALIFORNIA
BERKELEY, CALIFORNIA 94720